Multi-Aperture Space-Time Transmit and Receive Design for MIMO Radar

Xudong Zhang, *Graduate Student Member, IEEE*, Fangzhou Wang, and Hongbin Li, *Fellow, IEEE*

***Abstract*—We consider the joint transmit and receive design for multi-input multi-output radar with slow-time processing. The radar employs multiple transmit apertures to improve diversity. The design parameters include the spatial transmit code for each aperture, which varies from pulse to pulse to provide Doppler shaping, and the space-time receive filter, to jointly optimize the radar output signal-to-interference-and-noise ratio (SINR). To relieve the dependence on specific target parameters as required by some prior methods, we use the average SINR, averaged with respect to the target location/Doppler uncertainties, as the design metric. Simulation results show that our proposed multi-aperture solution outperforms a previous single-aperture based space-time transmit and receive design as well as the conventional phased-array radar.**

***Index Terms*—MIMO radar, space-time transmit and receive design, multi-aperture, average SINR.**

I. Introduction

In RECENT years, multi-input multi-output (MIMO) radar has been of significant interest owing to its unique advantages over phased-array radar [1]–[3], i.e., better target detection capability [4]–[7] and superior parameter estimation performance [8]–[11]. Joint transmit and receive design through maximizing the output signal-to-interference-and-noise ratio (SINR) is a key enabling technology.

Joint design can be performed by jointly optimizing the transmit waveform and receive filter using the prior target and clutter knowledge [12]. Along this direction, [13] proposed two sequential optimization algorithms to maximize the output SINR with constant-modulus and similarity constraints by using semidefinite relaxation (SDR). A different design which relaxes the constant-modulus constraint by a peak-to-average power ratio constraint was considered in [14]. Joint waveform and receive design for slow-moving target detection in clutter using space-time adaptive processing was examined in a number of works via cyclic optimization [15], mutual information maximization [16], and worst-case optimization [17]. In contrast, [18] proposed a joint design of the space-time transit code and receive filter, assuming all transmitters employ the same waveform. Moreover, the joint design problem can be pursued only in the spatial domain. Increasing the number of transmit apertures brings more degrees of freedom for interference suppression [3]. Transmit aperture optimization under a power constraint was investigated in [19], while [20] considered a similar problem with an additional similarity constraint with respect to (w.r.t.) some desired transmit beam patterns.

Similar to [18], we consider a space-time transmit and receive design problem for MIMO radar. A major distinction is that, while [18] uses a single aperture for transmission, we incorporate multiple apertures in the design. To relieve the dependence on specific target parameters as required by most prior studies, we use the average SINR, averaged w.r.t. the target location/Doppler uncertainties, as the design metric. A sequential optimization algorithm is proposed to solve the joint design problem by iteratively optimizing the SINR w.r.t. the transmit code and receive filter. The optimization w.r.t. the multi-aperture transmit code is converted into a fractional programming (FP) problem by using a semidefinite programming (SDP) based approximation. The FP problem is solved by Dinkelbach's algorithm, which is followed by a randomization procedure to obtain the optimum transmit code. The simulation results show that our proposed method converges in a few iterations and outperforms the single-aperture scheme [18] in terms of the average output SINR.

II. Signal Model

A MIMO radar consisting of N_{t} transmit antennas (TXs) and N_{r} receive antennas (RXs) was considered in [18]. Each TX emits a slow-time coded coherent train of K pulses. Let $\boldsymbol{b}_k = [b_1(k), \ldots, b_{N_{\mathrm{t}}}(k)]^T \in \mathbb{C}^{N_{\mathrm{t}}\times 1}$ denote a complex space-time code for the k-th pulse, $k = 1, \ldots, K$, where $(\cdot)^T$ denotes the transpose. Suppose there is a moving target at an azimuth angle θ_0. At the RX, the received signal is down-converted, matched-filtered, and sampled at the pulse rate. The output can be expressed as [18]

$$\widetilde{\boldsymbol{y}}_k = \alpha_0 e^{j2\pi(k-1)v_0}\boldsymbol{a}_{\mathrm{r}}(\theta_0)\boldsymbol{a}_{\mathrm{t}}^T(\theta_0)\boldsymbol{b}_k + \widetilde{\boldsymbol{d}}_k + \widetilde{\boldsymbol{n}}_k, \qquad (1)$$

where $\widetilde{\boldsymbol{d}}_k$ donates the clutter, $\widetilde{\boldsymbol{n}}_k$ the noise, α_0 the complex target amplitude, v_0 the normalized target Doppler frequency, while $\boldsymbol{a}_{\mathrm{t}}(\theta_0) \in \mathbb{C}^{N_{\mathrm{t}}\times 1}$ and $\boldsymbol{a}_{\mathrm{r}}(\theta_0) \in \mathbb{C}^{N_{\mathrm{r}}\times 1}$ denote the transmit and receive steering vector. For uniform linear array (ULA), the steering vector $\boldsymbol{a}_{\mathrm{t}}(\theta_0) = [1, e^{-j\pi\sin\theta_0}, \ldots, e^{-j\pi(N_{\mathrm{t}}-1)\sin\theta_0}]^T$ and $\boldsymbol{a}_{\mathrm{r}}(\theta_0)$ is similarly defined.

Unlike the single-aperture system in [18], we consider a MIMO radar that employs $M (M \leq N_{\mathrm{t}})$ transmit apertures using M orthogonal waveforms. For the m-th aperture, the TXs transmit a space-time code $\boldsymbol{b}_{m,k} \in \mathbb{C}^{N_{\mathrm{t}}\times 1}$ during the k-th pulse. A set of matched-filters are used at the receivers to separate signals from different apertures. Then, the received signal associated

Manuscript received February 9, 2021; revised March 28, 2021; accepted April 8, 2021. Date of publication April 16, 2021; date of current version May 24, 2021. This work was supported in part by the National Science Foundation under Grant ECCS-1609393 and Grant ECCS-1923739. The associate editor coordinating the review of this manuscript and approving it for publication was Prof. Jun Liu. *(Corresponding author: Hongbin Li.)*

The authors are with the Department of Electrical and Computer Engineering, Stevens Institute of Technology, Hoboken, NJ 07030 USA (e-mail: xzhan24@stevens.edu; fwang11@stevens.edu; hli@stevens.edu).

Digital Object Identifier 10.1109/LSP.2021.3072829

with the m-th aperture can be written as

$$\boldsymbol{y}_{m,k} = \alpha_0 e^{j2\pi(k-1)v_0} \boldsymbol{a}_{\text{r}}(\theta_0)\boldsymbol{a}_{\text{t}}^T(\theta_0)\boldsymbol{b}_{m,k} + \boldsymbol{d}_{m,k} + \boldsymbol{n}_{m,k},$$

where $\boldsymbol{d}_{m,k}$ is the clutter and $\boldsymbol{n}_{m,k}$ is the noise. By stacking the M outputs $\boldsymbol{y}_{m,k}$ into a vector $\boldsymbol{y}_k = [\boldsymbol{y}_{1,k}^T, \ldots, \boldsymbol{y}_{M,k}^T]^T$, we have

$$\boldsymbol{y}_k = \alpha_0 e^{j2\pi(k-1)v_0} \mathbf{A}(\theta_0)\boldsymbol{b}_k + \boldsymbol{d}_k + \boldsymbol{n}_k, \tag{2}$$

where $\mathbf{A}(\theta_0) = \mathbf{I}_M \otimes [\boldsymbol{a}_{\text{r}}(\theta_0)\boldsymbol{a}_{\text{t}}^T(\theta_0)]$, $\otimes$ denotes the Kronecker product, $\mathbf{I}_M$ the $M \times M$ identity matrix, and $\boldsymbol{b}_k$, $\boldsymbol{d}_k$, $\boldsymbol{n}_k$ are similarly formed from $\boldsymbol{b}_{m,k}$, $\boldsymbol{d}_{m,k}$, and $\boldsymbol{n}_{m,k}$. Let $\boldsymbol{y} = [\boldsymbol{y}_1^T, \ldots, \boldsymbol{y}_K^T]^T$. The received signals becomes

$$\boldsymbol{y} = \alpha_0 \mathbf{P}(\theta_0, v_0)\boldsymbol{b} + \boldsymbol{d} + \boldsymbol{n}, \tag{3}$$

where $\mathbf{P}(\theta_0, v_0) = \text{Diag}(\boldsymbol{p}(v_0)) \otimes \mathbf{A}(\theta_0)$, $\text{Diag}(\boldsymbol{p}(v_0))$ denotes a diagonal matrix formed by the temporal steering vector $\boldsymbol{p}(v_0) = [1, e^{j2\pi v_0}, \ldots, e^{j2\pi(K-1)v_0}]^T$, and $\boldsymbol{b}, \boldsymbol{d}, \boldsymbol{n}$ are similarly formed from $\boldsymbol{b}_k$, $\boldsymbol{d}_k$, and $\boldsymbol{n}_k$.

A space-time receive filter $\boldsymbol{w} \in \mathbb{C}^{N_{\text{r}}MK\times 1}$ is used to filter the received signal $\boldsymbol{y}$. The output can be expressed as

$$z = \boldsymbol{w}^H\boldsymbol{y} = \alpha_0 \boldsymbol{w}^H \mathbf{P}(\theta_0, v_0)\boldsymbol{b} + \boldsymbol{w}^H\boldsymbol{d} + \boldsymbol{w}^H\boldsymbol{n}, \tag{4}$$

where $(\cdot)^H$ denotes the conjugate transpose. The problem of interest is to jointly design $\boldsymbol{b}$ and $\boldsymbol{w}$.

III. Proposed Approach

In this section, we first introduce the design criterion, the average output SINR, for the joint design of the multi-aperture code $\boldsymbol{b}$ and receive filter $\boldsymbol{w}$ in (4). Then, a sequential procedure is proposed to iteratively optimize the average SINR w.r.t. $\boldsymbol{w}$ and $\boldsymbol{b}$.

A. Average Output SINR

Since the target parameters θ_0 and v_0 are usually unknown, we propose to employ the average SINR as the design metric

$$\rho(\boldsymbol{b}, \boldsymbol{w}) = \frac{\sigma_0^2 \mathbb{E}[|\boldsymbol{w}^H\mathbf{P}(\theta_0, v_0)\boldsymbol{b}|^2]}{\mathbb{E}[|\boldsymbol{w}^H\boldsymbol{d}|^2] + \boldsymbol{w}^H\mathbf{R}\boldsymbol{w}}, \tag{5}$$

where θ_0, v_0, and α_0 are modeled as independent random variables. $\sigma_0^2 = \mathbb{E}[|\alpha_0|^2]$ and $\mathbf{R}$ is the noise covariance matrix. The clutter $\boldsymbol{d} = \sum_{l=1}^{L} \alpha_l \mathbf{P}(\theta_l, v_l)\boldsymbol{b}$ consists of echoes from L scatterers located at θ_l with complex amplitudes α_l and normalized Doppler v_l, where α_l, θ_l, and v_l are modeled as uncorrelated random variables [12]. Hence, the average SINR becomes

$$\rho(\boldsymbol{b}, \boldsymbol{w}) = \frac{\boldsymbol{w}^H\boldsymbol{\Gamma}_b\boldsymbol{w}}{\boldsymbol{w}^H\boldsymbol{\Theta}_b\boldsymbol{w} + \boldsymbol{w}^H\mathbf{R}\boldsymbol{w}} = \frac{\boldsymbol{b}^H\boldsymbol{\Gamma}_w\boldsymbol{b}}{\boldsymbol{b}^H\boldsymbol{\Theta}_w\boldsymbol{b} + \boldsymbol{w}^H\mathbf{R}\boldsymbol{w}}, \tag{6}$$

where $\boldsymbol{\Gamma}_b$ and $\boldsymbol{\Theta}_b$ are $N_{\text{r}}MK \times N_{\text{r}}MK$ covariance matrices depending on $\boldsymbol{b}$, while $\boldsymbol{\Gamma}_w$ and $\boldsymbol{\Theta}_w$ are $N_{\text{t}}MK \times N_{\text{t}}MK$ covariance matrices depending on $\boldsymbol{w}$. The explicit expressions for $\boldsymbol{\Gamma}_b$ and $\boldsymbol{\Gamma}_w$ as well as $\boldsymbol{\Theta}_b$ and $\boldsymbol{\Theta}_w$ are given by (16) and, respectively, (23) in Appendix A.

B. Proposed Design

The joint design problem seeks to maximize the average SINR under a joint energy and constant-modulus constraint:

$$\begin{aligned} \max_{\boldsymbol{b},\boldsymbol{w}} \quad & \rho(\boldsymbol{b}, \boldsymbol{w}) \\ \text{s.t.} \quad & |\boldsymbol{b}(n)| = 1/\sqrt{N_{\text{t}}MK},\ n = 1, \ldots, N_{\text{t}}MK. \end{aligned} \tag{7}$$

Next, we propose an alternating method that sequentially and iteratively optimizes the average SINR w.r.t. $\boldsymbol{w}$ and $\boldsymbol{b}$.

1) Receive Filter Design: We first optimize the receive filter $\boldsymbol{w}$ by fixing the transmit code $\boldsymbol{b}$ to the one obtained from the ℓ-th iteration $\boldsymbol{b}^{(\ell)}$. Then, problem (7) becomes

$$\max_{\boldsymbol{w}} \quad \frac{\boldsymbol{w}^H\boldsymbol{\Gamma}_b^{(\ell)}\boldsymbol{w}}{\boldsymbol{w}^H\boldsymbol{\Theta}_b^{(\ell)}\boldsymbol{w} + \boldsymbol{w}^H\mathbf{R}\boldsymbol{w}}, \tag{8}$$

whose solution $\boldsymbol{w}^{(\ell+1)}$ is the eigenvector corresponding to the largest eigenvalue of the matrix $(\boldsymbol{\Theta}_b^{(\ell)} + \mathbf{R})^{-1}\boldsymbol{\Gamma}_b^{(\ell)}$.

2) Multi-Aperture Transmit Code Design: By fixing $\boldsymbol{w}$ to $\boldsymbol{w}^{(\ell+1)}$, problem (7) can be rewritten as

$$\begin{aligned} \max_{\boldsymbol{b}} \quad & \frac{\boldsymbol{b}^H\boldsymbol{\Gamma}_w^{(\ell+1)}\boldsymbol{b}}{\boldsymbol{b}^H\boldsymbol{\Theta}_w^{(\ell+1)}\boldsymbol{b} + \left(\boldsymbol{w}^{(\ell+1)}\right)^H\mathbf{R}\boldsymbol{w}^{(\ell+1)}} \\ \text{s.t.} \quad & |\boldsymbol{b}(n)| = 1/\sqrt{N_{\text{t}}MK},\ n = 1, \ldots, N_{\text{t}}MK, \end{aligned} \tag{9}$$

which is non-convex and can be relaxed into an SDP problem:

$$\begin{aligned} \max_{\mathbf{B}} \quad & \frac{\text{tr}(\boldsymbol{\Gamma}_w^{(\ell+1)}\mathbf{B})}{\text{tr}(\boldsymbol{\Theta}_w^{(\ell+1)}\mathbf{B}) + \left(\boldsymbol{w}^{(\ell+1)}\right)^H\mathbf{R}\boldsymbol{w}^{(\ell+1)}} \\ \text{s.t.} \quad & \text{Diag}(\mathbf{B}) = \mathbf{I}_{N_{\text{t}}MK}/(N_{\text{t}}MK),\ \ \mathbf{B} \succcurlyeq \mathbf{0}, \end{aligned} \tag{10}$$

where $\mathbf{B} = \boldsymbol{b}\boldsymbol{b}^H$ and $\mathbf{B} \succcurlyeq \mathbf{0}$ indicates that $\mathbf{B}$ is a positive semidefinite matrix. Problem (10) is a FP problem that can be solved by Dinkelbach's algorithm [21], [22]. Specifically, by introducing a slack variable ζ, (10) can be converted into

$$\begin{aligned} \max_{\mathbf{B},\zeta} \quad & f(\mathbf{B}) - \zeta g(\mathbf{B}) \\ \text{s.t.} \quad & \text{Diag}(\mathbf{B}) = \mathbf{I}_{N_{\text{t}}MK}/(N_{\text{t}}MK),\ \ \mathbf{B} \succcurlyeq \mathbf{0}, \end{aligned} \tag{11}$$

where $f(\mathbf{B})$ represents the numerator of the ratio in (10), $g(\mathbf{B})$ corresponds to the denominator. Problem (11) can be solved with an inner iteration which sequentially and iteratively maximizes the objective function w.r.t. $\mathbf{B}$ and ζ.

Denote the slack variable ζ at the ℓ_1-th inner iteration as $\zeta^{(\ell_1)}$. Then, the matrix $\mathbf{B}^{(\ell_1+1)}$ can be obtained by solving

$$\begin{aligned} \max_{\mathbf{B}} \quad & f(\mathbf{B}) - \zeta^{(\ell_1)} g(\mathbf{B}) \\ \text{s.t.} \quad & \text{Diag}(\mathbf{B}) = \mathbf{I}_{N_{\text{t}}MK}/(N_{\text{t}}MK),\ \ \mathbf{B} \succcurlyeq \mathbf{0}, \end{aligned} \tag{12}$$

which is a convex problem and can be solved through standard numerical solvers, e.g., CVX [23]. Once the solution for (12) is obtained, we can update the slack variable $\zeta^{(\ell_1+1)}$ for the $(\ell_1 + 1)$-st iteration by

$$\zeta^{(\ell_1+1)} = \frac{f(\mathbf{B}^{(\ell_1+1)})}{g(\mathbf{B}^{(\ell_1+1)})}. \tag{13}$$

The slack variable ζ is initialized as 0 for each inner iteration and the iterative process of Dinkelbach's algorithm ends when

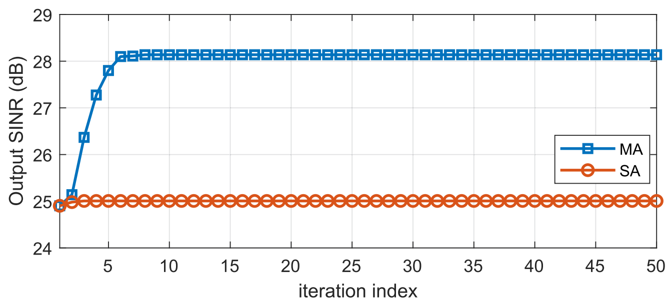

Fig. 1. Convergence behavior of the proposed method.

the improvement of the cost function of (11) over two adjacent iterations is smaller than a tolerance δ, i.e. $\delta = 10^{-3}$.

After solving (10), we need to convert the optimal solution $\mathbf{B}^{(\ell+1)}$ into a feasible solution $\boldsymbol{b}^{(\ell+1)}$ to (9). A randomization method can be used to obtain a solution $\boldsymbol{b}^{(\ell+1)}$ from $\mathbf{B}^{(\ell+1)}$ [24]. Consider a random complex vector $\boldsymbol{\xi}$ with zero-mean and covariance matrix $\mathbf{B}^{(\ell+1)}$. It is easy to show that (12) is equivalent to the following stochastic optimization problem

$$\max_{\mathbb{E}[\boldsymbol{\xi}\boldsymbol{\xi}^H]} \ \mathbf{F}(\boldsymbol{\xi}) \quad \text{s.t. } \mathbb{E}[\text{Diag}(\boldsymbol{\xi}\boldsymbol{\xi}^H)] = \mathbf{I}_{N_{\text{t}}MK}/(N_{\text{t}}MK), \quad \mathbb{E}[\boldsymbol{\xi}\boldsymbol{\xi}^H] \succcurlyeq \mathbf{0}, \tag{14}$$

where $\mathbf{F}(\boldsymbol{\xi}) = \mathbb{E}[\boldsymbol{\xi}\boldsymbol{\Gamma}_w^{(\ell+1)}\boldsymbol{\xi}^H] - \zeta^{(\ell_1)}(\mathbb{E}[\boldsymbol{\xi}\boldsymbol{\Theta}_w^{(\ell+1)}\boldsymbol{\xi}^H] + (\boldsymbol{w}^{(\ell+1)})^H\mathbf{R}\boldsymbol{w}^{(\ell+1)})$. Hence, the stochastic interpretation of the SDR in (14) allows us to obtain an approximate rank-one solution to (9). Specifically, given $\mathbf{B}^{(\ell_1+1)}$, we can generate a set of independent and identically distributed complex Gaussian random vectors $\boldsymbol{\xi}_i \sim \mathcal{CN}(0, \mathbf{B}^{(\ell_1+1)}), i = 1, \ldots, Q$, where Q is the number of randomization trials. Then, a rank-one solution is obtained as

$$\boldsymbol{b}^{(\ell+1)} = \arg\max_{\widetilde{\boldsymbol{\xi}}_i} \frac{\widetilde{\boldsymbol{\xi}}_i^H \boldsymbol{\Gamma}_w^{(\ell+1)} \widetilde{\boldsymbol{\xi}}_i}{\widetilde{\boldsymbol{\xi}}_i^H \boldsymbol{\Theta}_w^{(\ell+1)} \widetilde{\boldsymbol{\xi}}_i + \left(\boldsymbol{w}^{(\ell+1)}\right)^H \mathbf{R}\boldsymbol{w}^{(\ell+1)}}, \tag{15}$$

where $\widetilde{\boldsymbol{\xi}}_i(n) = \boldsymbol{\xi}_i(n)/(|\boldsymbol{\xi}_i(n)|\sqrt{N_{\text{t}}MK})$, $n = 1, \ldots, N_{\text{t}}MK$. Simulation results show that $Q = 1000$ is generally sufficient to yield a good solution.

The proposed sequential algorithm is detailed in **Algorithm** 1. The computational complexity for **Algorithm** 1 is mainly due to the generalized eigenvalue decomposition in Step 1), solving the convex problem in Step 3a), and randomization in Step 6), which have a complexity of $\mathcal{O}(N_{\text{r}}MK)^3$, $\mathcal{O}(N_{\text{t}}MK)^{3.5}$, and $\mathcal{O}(Q(N_{\text{t}}MK)^2)$, respectively [25].

Algorithm 1: The Proposed Sequential Algorithm.

Input: Known parameters that define problem (7).
Output: The receive filter $\boldsymbol{w}$ and the transmit code $\boldsymbol{b}$.
Initialization: Initialize $\boldsymbol{b}^{(0)}$ and set $\ell = 1$.
repeat
1) Update $\boldsymbol{w}^{(\ell)}$ by solving (8).
2) Initialize $\zeta^{(0)} = 0$ and set iteration index $\ell_1 = 1$.
3) **repeat**
  a) Solve for $\mathbf{B}^{(\ell_1+1)}$ by using (12).
  b) Update $\zeta^{(\ell_1+1)}$ with (13).
  c) Set $\ell_1 = \ell_1 + 1$.
4) **until** convergence.
5) **return** $\mathbf{B}^{(\ell+1)} = \mathbf{B}^{(\ell_1)}$.
6) Apply randomization to obtain $\boldsymbol{b}^{(\ell+1)}$ by using (15).
7) Set $\ell = \ell + 1$.
until convergence.
return $\boldsymbol{w} = \boldsymbol{w}^{(\ell)}$ and $\boldsymbol{b} = \boldsymbol{b}^{(\ell)}$.

IV. Results

In this section, the performance of the proposed joint design is investigated via numerical simulations. We consider a colocated MIMO radar with $N_{\text{t}} = 5$ TXs and $N_{\text{r}} = 3$ RXs. We set the code length $K = 10$ and a total of $M = 4$ transmit apertures are used. The Doppler frequencies and azimuth angles for the target and the clutter are generated by using the statistic models described in Appendix A. In the simulation, unless otherwise specified, the target mean azimuth and Doppler are $\bar{\theta}_0 = 5^\circ$ and $\bar{v}_0 = 0.15$ with uncertainty intervals $\vartheta_0 = 2^\circ$ and $\varepsilon_0 = 0.04$, respectively. Following a standard space-time clutter model [26], the clutter is generated from $L = 20$ scatterers which are uniformly located along the diagonal clutter ridge of the Doppler-azimuth plane. Like the target model, the clutter model includes similar azimuth/Doppler uncertainty intervals for each clutter scatterer (see Appendix A). In addition, we assume the noise $\boldsymbol{n}$ is a zero-mean circular complex Gaussian random vector with covariance matrix $\mathbf{R} = \sigma^2\mathbf{I}_{N_{\text{r}}MK}$ and $\sigma^2 = 0.01$. The target and clutter powers are $\sigma_0^2 = 10$ dB and, respectively, $\sigma_l^2 = 30$ dB, or varied over a range of values as specified.

We consider the performance of the following methods:

- **MA**: The proposed multi-aperture joint transmit-receive design for MIMO radar.
- **SA**: The single-aperture joint transmit-receive design for MIMO radar [18].
- **PA**: The conventional phased-array radar with a single transmit aperture and a minimum variance distortionless response based receiver.

Note that an initialization of the transmit code is required. In the simulation, $\boldsymbol{b}$ is initialized as a normalized all-one vector with unit energy $||\boldsymbol{b}||^2 = 1$ for both MA and SA. Moreover, every $\boldsymbol{b}_k$ for PA is fixed to be the conjugate of $\boldsymbol{a}_{\text{t}}(\bar{\theta}_0)$.

We first examine the convergence of the proposed method. Fig. 1 shows that the SA converges faster, due to its smaller problem size, than the MA, and both methods converge within a small number of iterations, e.g., less than 10 iterations. Moreover, the MA offers about 3 dB improvement over the SA method.

Next, we consider the output SINR versus the target and clutter power. Fig. 2 (a) shows that the output SINR of all considered methods increases when the target power increases, with MA being the best. We see as the clutter power increases, the output SINR decreases and the gap between the MA and SA becomes larger, which indicates that the MA can better cope with stronger clutter. This is because the MA offers more degrees of freedom for clutter suppression.

Finally, we evaluate the effects of the clutter azimuth and Doppler uncertainties. Fig. 2 (c) and (d) show the output SINR versus the clutter azimuth uncertainty interval ϑ_0 and,

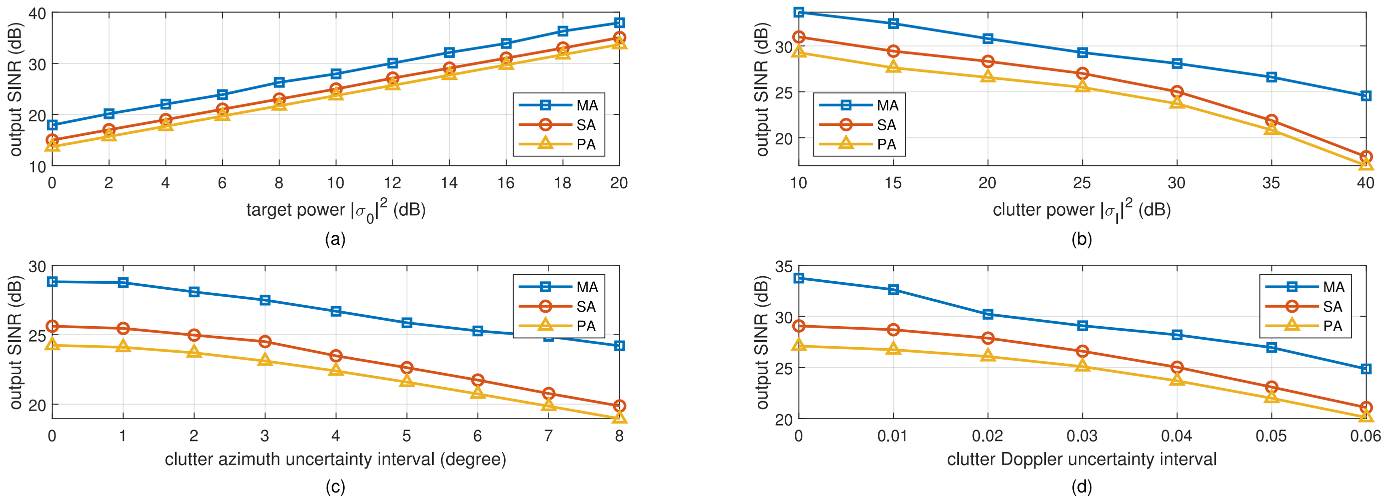

Fig. 2. Output SINR versus (a) target power, (b) clutter power, (c) clutter azimuth uncertainty, and (d) clutter Doppler uncertainty.

respectively, clutter Doppler uncertainty interval ε_0. The results show that the output SINR decreases as the uncertainty intervals increase due to the increasing inaccuracy on the knowledge of the clutter. Moreover, the MA still outperforms the SA even with a large clutter uncertainty level.

V. Conclusions

We proposed a joint design of the space-time transmit code and the receive filter in a multi-aperture MIMO radar by maximizing the average radar output SINR. The resulting non-convex optimization problem was solved in an sequential and iterative manner along with FP and SDP techniques. The results show that our proposed multi-aperture approach outperforms the single-aperture joint transmit and receive design for MIMO radar as well as the conventional phased-array radar.

Appendix A
Calculation of Covariance Matrices in (6)

$\mathbf{\Gamma}_b$ and $\mathbf{\Gamma}_w$ can be rewritten in block matrix forms as

$$\mathbf{\Gamma}_b = (\sigma_0^2 \mathbf{\Gamma}_b^{k_1,k_2})_{K\times K}, \quad \mathbf{\Gamma}_w = (\sigma_0^2 \mathbf{\Gamma}_w^{k_1,k_2})_{K\times K}, \tag{16}$$

where the sub-matrices $\mathbf{\Gamma}_b^{k_1,k_2} \in \mathbb{C}^{MN_\text{r}\times MN_\text{r}}$ and $\mathbf{\Gamma}_w^{k_1,k_2} \in \mathbb{C}^{MN_\text{t}\times MN_\text{t}}$ for $k_1, k_2 = 1,\ldots,K$. By treating the target Doppler v_0 and angle θ_0 as independent random variables, the block matrices $\mathbf{\Gamma}_b^{k_1,k_2}$ and $\mathbf{\Gamma}_w^{k_1,k_2}$ can be expressed as

$$\mathbf{\Gamma}_b^{k_1,k_2} = \mathbb{E}[e^{j2\pi(k_1-k_2)v_0}]\mathbb{E}[\mathbf{A}(\theta_0)\boldsymbol{b}_{k_1}\boldsymbol{b}_{k_2}^H\mathbf{A}^H(\theta_0)], \tag{17}$$

$$\mathbf{\Gamma}_w^{k_1,k_2} = \mathbb{E}[e^{-j2\pi(k_1-k_2)v_0}]\mathbb{E}[\mathbf{A}^H(\theta_0)\boldsymbol{w}_{k_1}\boldsymbol{w}_{k_2}^H\mathbf{A}(\theta_0)], \tag{18}$$

where $\boldsymbol{w}_k$ denotes the receive filter for the k-th pulse. The target Doppler v_0 is assumed to be uniformly distributed: $v_0 \sim \mathcal{U}(\bar{v}_0 - \frac{\varepsilon_0}{2}, \bar{v}_0 + \frac{\varepsilon_0}{2})$. Then, the first expectation of (17) becomes

$$\mathbb{E}[e^{j2\pi(k_1-k_2)v_0}] = e^{j2\pi\bar{v}_0(k_1-k_2)}\text{sinc}[\pi\varepsilon_0(k_1-k_2)]. \tag{19}$$

By defining matrix $\mathbf{B}_k = [\boldsymbol{b}_{1,k},\ldots,\boldsymbol{b}_{M,k}]$, we have

$$\mathbf{A}(\theta_0)\boldsymbol{b}_k = \left(\mathbf{B}_k^T \otimes \mathbf{I}_{N_\text{r}}\right)\left(\boldsymbol{a}_\text{t}(\theta_0)\otimes \boldsymbol{a}_\text{r}(\theta_0)\right), \tag{20}$$

and the second expectation of (17) can be written as

$$\mathbb{E}[\mathbf{A}(\theta_0)\boldsymbol{b}_{k_1}\boldsymbol{b}_{k_2}^H\mathbf{A}^H(\theta_0)] = \left(\mathbf{B}_{k_1}^T\otimes\mathbf{I}_{N_\text{r}}\right)\mathbf{\Psi}\left(\mathbf{B}_{k_2}^T\otimes\mathbf{I}_{N_\text{r}}\right)^H,$$
$$\mathbf{\Psi} = \int_{\bar{\theta}_0-\frac{\vartheta_0}{2}}^{\bar{\theta}_0+\frac{\vartheta_0}{2}} \left(\boldsymbol{a}_\text{t}(\theta_0)\boldsymbol{a}_\text{t}^H(\theta_0)\right)\otimes\left(\boldsymbol{a}_\text{r}(\theta_0)\boldsymbol{a}_\text{r}^H(\theta_0)\right)d\theta_0. \tag{21}$$

The target azimuth θ_0 is also assumed to be uniformly distributed: $\theta_0 \sim \mathcal{U}(\bar{\theta}_0 - \frac{\vartheta_0}{2}, \bar{\theta}_0 + \frac{\vartheta_0}{2})$. $\mathbf{\Psi}$ can be partitioned into $N_\text{t}\times N_\text{t}$ blocks, each of which is an $N_\text{r}\times N_\text{r}$ sub-matrix. Denoting $\mathbf{\Psi}_{q_1q_2}^{p_1p_2}$ as the (p_1,p_2)-th entry of the (q_1,q_2)-th block of $\mathbf{\Psi}$, we have

$$\mathbf{\Psi}_{q_1q_2}^{p_1p_2} = \frac{1}{\vartheta_0}\int_{\bar{\theta}_0-\frac{\vartheta_0}{2}}^{\bar{\theta}_0+\frac{\vartheta_0}{2}} e^{-j\pi\sin\theta_0[(q_1-q_2)+(p_1-p_2)]}d\theta_0. \tag{22}$$

Similarly, $\mathbf{\Gamma}_w$ can be calculated by following the derivation of $\mathbf{\Gamma}_b$. The first part of the expectation in (18) can be obtained from the conjugate of the matrix in (19). To compute the second expectation of (18), we define a matrix $\mathbf{W}_k = [\boldsymbol{w}_{1,k},\ldots,\boldsymbol{w}_{M,k}]$ with $\boldsymbol{w}_{m,k}\in\mathbb{C}^{N_\text{r}\times 1}$ as the filter for the m-th aperture of the k-th pulse. Then, we have

$$\mathbb{E}[\mathbf{A}^H(\theta_0)\boldsymbol{w}_{k_1}\boldsymbol{w}_{k_2}^H\mathbf{A}(\theta_0)] = \left(\mathbf{W}_{k_1}^T\otimes\mathbf{I}_{N_\text{t}}\right)\widetilde{\mathbf{\Psi}}\left(\mathbf{W}_{k_2}^T\otimes\mathbf{I}_{N_\text{t}}\right)^H,$$
$$\widetilde{\mathbf{\Psi}} = \int_{\bar{\theta}_0-\frac{\vartheta_0}{2}}^{\bar{\theta}_0+\frac{\vartheta_0}{2}} \left(\boldsymbol{a}_\text{r}^*(\theta_0)\boldsymbol{a}_\text{r}^T(\theta_0)\right)\otimes\left(\boldsymbol{a}_\text{t}^*(\theta_0)\boldsymbol{a}_\text{t}^T(\theta_0)\right)d\theta_0,$$

which can be similarly obtained as in (22).

The clutter azimuth θ_l and Doppler v_l are assumed to be independent and uniformly distributed variables with mean $\bar{\theta}_l$, $\bar{v}_l$ and uncertainty intervals $\vartheta_l, \varepsilon_l$. Then, the covariance matrices $\mathbf{\Theta}_b$ and $\mathbf{\Theta}_w$ can be written as

$$\mathbf{\Theta}_b = \sum_{l=1}^{L}\sigma_l^2\mathbf{\Theta}_{b,l}, \quad \mathbf{\Theta}_w = \sum_{l=1}^{L}\sigma_l^2\mathbf{\Theta}_{w,l}, \tag{23}$$

where $\sigma_l^2 = \mathbb{E}[|\alpha_l|^2]$. Note that matrices $\mathbf{\Theta}_{b,l}$ and $\mathbf{\Theta}_{w,l}$ can be similarly obtained from (16) by replacing θ_0 and v_0 with θ_l and v_l, respectively.

REFERENCES

[1] J. Li and P. Stoica, *MIMO Radar Signal Processing*. Hoboken, NJ, USA: Wiley, 2008.

[2] A. M. Haimovich, R. S. Blum, and L. J. Cimini, “MIMO radar with widely separated antennas,” *IEEE Signal Process. Mag.*, vol. 25, no. 1, pp. 116–129, Jan. 2008.

[3] H. Li and B. Himed, “Transmit subaperturing for MIMO radars with co-located antennas,” *IEEE J. Sel. Topics Signal Process.*, vol. 4, no. 1, pp. 55–65, Feb. 2010.

[4] Z. Cheng, B. Liao, Z. He, J. Li, and C. Han, “A nonlinear-ADMM method for designing MIMO radar constant modulus waveform with low correlation sidelobes,” *Signal Process.*, vol. 159, pp. 93–103, Jun. 2019.

[5] J. Liu and J. Li, “Robust detection in MIMO radar with steering vector mismatches,” *IEEE Trans. Signal Process.*, vol. 67, no. 20, pp. 5270–5280, Oct. 2019.

[6] Y. Li, Q. He, and R. S. Blum, “Limited-complexity receiver design for passive/active MIMO radar detection,” *IEEE Trans. Signal Process.*, vol. 67, no. 12, pp. 3258–3271, Jun. 2019.

[7] P. Wang and H. Li, “Target detection with imperfect waveform separation in distributed MIMO radar,” *IEEE Trans. Signal Process.*, vol. 68, pp. 793–807, 2020.

[8] N. Garcia, H. Wymeersch, E. G. Larsson, A. M. Haimovich, and M. Coulon, “Direct localization for massive MIMO,” *IEEE Trans. Signal Process.*, vol. 65, no. 10, pp. 2475–2487, May 2017.

[9] B. Liao, “Fast angle estimation for MIMO radar with nonorthogonal waveforms,” *IEEE Trans. Aerosp. Electron. Syst.*, vol. 54, no. 4, pp. 2091–2096, Aug. 2018.

[10] R. Amiri, F. Behnia, and M. A. M. Sadr, “Exact solution for elliptic localization in distributed MIMO radar systems,” *IEEE Trans. Veh. Technol.*, vol. 67, no. 2, pp. 1075–1086, Feb. 2018.

[11] Y. Gu and Y. D. Zhang, “Compressive sampling optimization for user signal parameter estimation in massive MIMO systems,” *Digit. Signal Process.*, vol. 94, pp. 105–113, Nov. 2019.

[12] A. Aubry, A. DeMaio, A. Farina, and M. Wicks, “Knowledge-aided (potentially cognitive) transmit signal and receive filter design in signal-dependent clutter,” *IEEE Trans. Aerosp. Electron. Syst.*, vol. 49, no. 1, pp. 93–117, Jan. 2013.

[13] G. Cui, H. Li, and M. Rangaswamy, “MIMO radar waveform design with constant modulus and similarity constraints,” *IEEE Trans. Signal Process.*, vol. 62, no. 2, pp. 343–353, Jan. 2014.

[14] Z. Cheng, Z. He, B. Liao, and M. Fang, “MIMO radar waveform design with PAPR and similarity constraints,” *IEEE Trans. Signal Process.*, vol. 66, no. 4, pp. 968–981, Feb. 2018.

[15] B. Tang and J. Tang, “Joint design of transmit waveforms and receive filters for MIMO radar space-time adaptive processing,” *IEEE Trans. Signal Process.*, vol. 64, no. 18, pp. 4707–4722, Sep. 2016.

[16] G. Sun, Z. He, J. Tong, X. Yu, and S. Shi, “Mutual information-based waveform design for MIMO radar space-time adaptive processing,” *IEEE Trans. Geosci. Remote Sens.*, vol. 59, no. 4, pp. 2909–2921, Apr. 2021.

[17] Y. Wang, W. Li, Q. Sun, and G. Huang, “Robust joint design of transmit waveform and receive filter for MIMO radar space-time adaptive processing with signal-dependent interferences,” *IET Radar, Sonar Navigat.*, vol. 11, no. 8, pp. 1321–1332, 2017.

[18] G. Cui, X. Yu, V. Carotenuto, and L. Kong, “Space-time transmit code and receive filter design for colocated MIMO radar,” *IEEE Trans. Signal Process.*, vol. 65, no. 5, pp. 1116–1129, Mar. 2017.

[19] J. Zhou, H. Li, and W. Cui, “Joint design of transmit and receive beamforming for transmit subaperturing MIMO radar,” *IEEE Signal Process. Lett.*, vol. 26, no. 11, pp. 1648–1652, Nov. 2019.

[20] Z. Cheng, B. Liao, Z. He, J. Li, and J. Xie, “Joint design of the transmit and receive beamforming in MIMO radar systems,” *IEEE Trans. Veh. Technol.*, vol. 68, no. 8, pp. 7919–7930, Aug. 2019.

[21] W. Dinkelbach, “On nonlinear fractional programming,” *Manage. Sci.*, vol. 13, no. 7, pp. 492–498, 1967.

[22] F. Wang and H. Li, “Joint waveform and receiver design for co-channel hybrid active-passive sensing with timing uncertainty,” *IEEE Trans. Signal Process.*, vol. 68, pp. 466–477, 2020.

[23] M. Grant and S. Boyd, “CVX: Matlab software for disciplined convex programming, version 2.1,” Mar. 2014.

[24] Z. Luo, W. Ma, A. M. So, Y. Ye, and S. Zhang, “Semidefinite relaxation of quadratic optimization problems,” *IEEE Signal Process. Mag.*, vol. 27, no. 3, pp. 20–34, May 2010.

[25] S. Boyd and L. Vandenberghe, *Convex Optimization*, Cambridge, U.K: Cambridge Univ. Press, 2004.

[26] J. Ward, “Space-time adaptive processing for airborne radar,” in *Proc. Int. Conf. Acoust., Speech, Signal Process.*, Massachusetts Inst. Technol. Lexington Lincoln Lab,1995, pp. 2809–2812.